



# Generalized distributions for modeling precipitation extremes based on the $L$ moment approach for the Amman Zara Basin, Jordan

Mohamad N. Ibrahim<sup>1</sup>

Received: 11 March 2018 / Accepted: 4 April 2019 / Published online: 10 May 2019  
© Springer-Verlag GmbH Austria, part of Springer Nature 2019

## Abstract

Extreme event magnitude and frequency are prerequisites for accurately designing and managing various water infrastructure systems. This paper studies precipitation extremes in the Amman Zara Basin (AZB) using daily precipitation records from 24 weather stations during a period that exceeds 50 years. Two extreme precipitation series (the annual maximum (AM) and the peak over threshold (POT)), four generalized probability distributions (generalized extreme value (GEV), generalized Pareto (GP), generalized lognormal (GLN), and generalized logistic (GLO)) and the  $L$  moment method for distribution parameter estimation are used. A mix of increasing and decreasing trends is observed at different stations for both the AM and POT series over the study period. Since the POT series considers up to the fifth largest precipitation in some years, in contrast to the AM series, and skips the largest precipitation in the AM series in other years, the trend analysis results for the POT series differ slightly from those for the AM series. According to the goodness-of-fit (Kolmogorov-Smirnov test and  $L$  moment diagram), the probability distributions GEV, GLN, and GLO can better fit the AM series, with no unique distribution among them consistently ranking the best for all stations, while the POT series is better fitted by the GP distribution. The calculated extreme precipitation amounts of the AM series are up to 18% greater than those of the POT series for the same return period. Additionally, the AM series can describe extreme precipitation events better than the POT series based on relative error calculations. The 50- and 100-year extreme precipitation events occurred more frequently in recent years.

**Keywords** Extreme precipitation · Generalized distributions ·  $L$  moment approach · Return period · Amman Zara Basin · Kolmogorov-Smirnov test · Mann-Kendall test

## 1 Introduction

Since as early as the middle of the last century, extreme hydrological events (i.e., high and low precipitation, flood and drought) have been an active research subject. Extreme event magnitude and frequency (return period) are prerequisites for accurately designing and managing various water infrastructure systems (including dam spillways, culverts, storm sewer systems, water supply systems, and flood control structures) and in climate change and flood risk assessment studies. In its fourth assessment report (IPCC 2007), the Intergovernmental Panel on Climate Change (IPCC) stated that, influenced by excessive greenhouse gas emissions, global temperatures are

likely to increase during the twenty-first century. This will probably result in changing of the hydrological cycle. Therefore, this changing climate is very likely to affect the frequency and intensity of extreme events. In recent years, a number of worldwide research studies have reported an increase in extreme precipitation events in terms of frequency and magnitude in most parts of the world, even in regions where there has been a decreasing trend in total precipitation (Arnone et al. 2013; Babar and Ramesh 2014; Douglas and Fairbank 2011; Groisman et al. 2005; Lenderink and van Meijgaard 2008; Ma et al. 2015; O’Gorman 2015).

Frequency analysis is a statistical technique that relates the magnitude of extreme events to their frequency of occurrence using an appropriate probability distribution function (Chow et al. 1988). In this technique, a historical precipitation series is used to select an appropriate probability distribution and its associated parameters. In the literature, the analysis of extreme events involves the use of annual maximum (AM) series (Adamowski 2000; Guru and Jha 2015; Li et al. 2016; Saf

✉ Mohamad N. Ibrahim  
m.najib@ttu.edu.jo; ibrahim6@buffalo.edu

<sup>1</sup> Department of Civil Engineering, Tafila Technical University,  
P.O. Box 179, Tafila 66110, Jordan

2009; She et al. 2013; Xia et al. 2012a, 2012b) and peaks over a threshold (POT) series (Adamowski 2000; Guru and Jha 2015; Li et al. 2014a, b, 2016; She et al. 2013; Xia et al. 2012a, 2012b), which are also known as partial duration (PD) series, as the most common extreme precipitation data series. While the AM series considers only the largest precipitation event in each year, the POT series involves more information about the extremes because the second or third largest precipitation amount may also cause extreme precipitation events in some years (Xia et al. 2012b). For data series with limited records, Madsen et al. (1997a) recommend using POT data series. Madsen et al. (1997b) and others (Zin and Jemain 2010) also recommend the use of POT data series since this approach could improve the parameter estimation of the probability distribution that represents the data.

Unfortunately, there is no unique probability distribution that can be implemented over other distributions for at-site or regional frequency analysis. Therefore, several possible theoretical probability distributions have been used or suggested to describe extreme precipitation amounts (e.g., extreme value type I, called the Gumbel; generalized extreme value (GEV); extreme value type III, called the Weibull; normal; lognormal; gamma; Pearson type 3; log Pearson type 3; exponential; generalized Pareto (GP); and Wakeby), of which the extreme value type I (Gumbel) distribution and log Pearson type 3 distribution have found widespread application in hydrological modeling (Haddad and Rahman 2011).

Al-hourri et al. (2014) indicated that the lognormal distribution provides a better fit than a linear distribution to the annual daily maximum precipitation in the Amman Zara Basin (AZB), Jordan. Zhi Li et al. (2014a) found that the skewed normal distribution performs the best among six probability distributions (exponential, gamma, Weibull, skewed normal, mixed exponential, and hybrid exponential/generalized Pareto) in reproducing extreme precipitation events on the Loess Plateau, China. However, Li et al. (2015) showed that the GEV, Burr, and Weibull distributions provide the best fit to both annual and seasonal maximum precipitation based on daily precipitation data at 13 stations in the Heihe River and Shiyang River basins. Beskow et al. (2015) compared four probability distributions (kappa, GEV, Grumbel, and lognormal) to identify the most appropriate distribution for the modeling of extreme precipitation events in southern Brazil. The GEV, among four other probability distributions, namely, the generalized logistic (GLO), Weibull, gamma, and lognormal distributions, represents the distribution with the most accurate seasonal maximum precipitation estimates for southern Quebec, Canada (Benyahya et al. 2014). Vahid Rahmani et al. (2014) used the Weibull distribution to calculate the extreme precipitation frequency using daily precipitation data (1920–2009) from 24 stations in Kansas and 15 stations from adjacent states. Some studies have used the GEV (Du et al. 2014; Madsen et al. 1997a, 1997b; Xia et al. 2012b) and

generalized GP (Du et al. 2014; Li et al. 2014a, b; Madsen et al. 1997a, 1997b; Xia et al. 2012b) distributions to analyze historical extreme precipitation events. Moreover, from these studies, the conclusion that the GEV is expected to fit AM series and that the GP is the expected distribution to better fit the POT series is supported. The appropriate probability distribution among candidate distributions is often selected by either statistical tests (the chi-square test, Kolmogorov-Smirnov (KS) test, Anderson-Darling test, Akaike information criterion or Bayesian information criterion) or graphical methods (the quantile-quantile plot or the  $L$  moment ratio diagram).

Since it was introduced by Hosking (1990), due to its theoretical advantages listed below in the data and methodology section, the  $L$  moment method has been increasingly used in hydrological frequency analysis for the estimation of probability distribution parameters rather than other standard methods, such as the moment method, maximum likelihood method, and least-squares method (Gubareva and Gartsman 2010; Li et al. 2014a, b; Rahman et al. 2013; She et al. 2013; Xia et al. 2012b; Yang et al. 2010; Zakaria et al. 2012). Additionally, this method has been widely used for regional flood (Adamowski 2000; Ellouze and Abida 2008; Noto and Loggia 2009; Saf 2009; Yang et al. 2010) and precipitation (Abolverdi and Khalili 2010; Hassan and Ping 2012; Parida and Moalafhi 2008; Zakaria et al. 2012) frequency analysis, for mapping extreme drought events (Núñez et al. 2011; She et al. 2013; Zin and Jemain 2010) and for low-flow studies (Chen et al. 2006).

Intensive storms often cause property damage and loss of life. The November 5, 2015 flash flood in the capital of Jordan, Amman, resulting from approximately 45 mm of precipitation over 40 min, caused four deaths and caused hundreds of vehicles to be washed away or left stranded. Additionally, as many as 20 families were left without houses. However, studies about precipitation frequency analysis and the selection of an appropriate probability distribution to fit available historical data have received very limited attention from researchers in Jordan. However, most of the precipitation data are not analyzed comprehensively. The focus in studies has been on the general aspects of precipitation (Dahamsheh and Aksoy 2007; Salahat and Al-qinna 2015) (pattern, trend, and variability) and climate change impact (Matouq et al. 2013; Salahat and Al-qinna 2015; Törnros and Menzel 2014) and adaptation scenarios. To the best of my knowledge, only the study performed by Al-hourri et al. (2014) has presented the application of the normal and lognormal distributions to fit only the AM data series in the AZB, Jordan. Accordingly, there is a need for reliable estimates of extreme precipitation events. Thus, the major objective of the present study was to examine the applicability of generalized probability distributions (GEV, GP, generalized lognormal (GLN), and GLO) to reliably represent the AM and POT data series at

each of a number of selected weather stations in AZB, Jordan. The method of *L* moments was applied for parameter estimation of each aforementioned distribution. The applicability of the probability distributions was measured by using the Kolmogorov-Smirnov goodness-of-fit test and the *L* moment ratio diagram. Special emphasis was placed on the investigation of extreme precipitation trends over time using the Mann-Kendall (M-K) test. A secondary objective was to determine the precipitation amount at each selected weather station for the AM and POT data series under return periods of 5, 10, 25, and 50 years based on the best-fitted distribution. The results of this research will provide valuable information and constitute the basis for future studies on extreme precipitation analysis and climate change assessments in the AZB.

## 2 Data and methodology

### 2.1 Study area and datasets

The Amman Zara Basin (AZB), located in the northwest part of Jordan between 213000 to 319000 east and 1140000 to 1220000 north (according to the Palestine grid), was selected as the study area. The total basin area is approximately 4150 km<sup>2</sup>, of which 3725 km<sup>2</sup> is located in Jordan, and the remaining area is in Syria (Fig. 1). The population density in AZB is relatively high, including the two largest urban cities in Jordan: Amman (the capital) and Zara. The AZB also contains most of Jordan’s commercial and industrial activities.

The elevation of the AZB ranges from 350 m below mean sea level at the Jordan River to 1100 m above mean sea level near Sweilih. The eastern margin of the basin is part of the desert plateau. Toward the west, the basin changes to highland

and then becomes progressively steeper until it reaches the Jordan valley.

Daily precipitation records from 24 weather stations spread across the AZB during a period that exceeds 50 years (1940–2015 for most stations), collected from the Ministry of Water and Irrigation in Jordan, were used in this study. The locations of these stations across the basin are shown in Fig. 1, with the reference station ID, station name, station coordinates, and statistical characteristics of each station given in Table 1. The selected stations have relatively complete records for the whole period.

The climate in AZB is considered a semiarid type with uneven spatial and temporal distributions of precipitation amounts. The bulk of this amount is concentrated between October and May (i.e., in the winter season). Statistically, the largest precipitation frequencies occur in January or February, with the maximum precipitation usually occurring in December or January. With decreasing altitude, the precipitation amount decreases toward the east from approximately 500 mm average annual precipitation in the west (Sweilih station) to approximately 100 mm in the east (Sabha and Subhiyeh station) (Table 1).

The coefficient of variation (CV), a statistic measuring the relative deviation from the average, is calculated in Table 1 based on annual precipitation and is an indicator of the inter-annual precipitation variation (i.e., year-to-year variability) throughout the basin. The spatial distribution of the CV, with values ranging from 0.32 to 0.51, indicates high interannual variability, which becomes more variable in the middle and east parts of the basin as aridity increases.

In this study, both the annual maximum (AM) series and the peak over threshold (POT) series are considered at each station. The AM series consists of the annual maximum daily precipitation, while the POT series contains all the daily

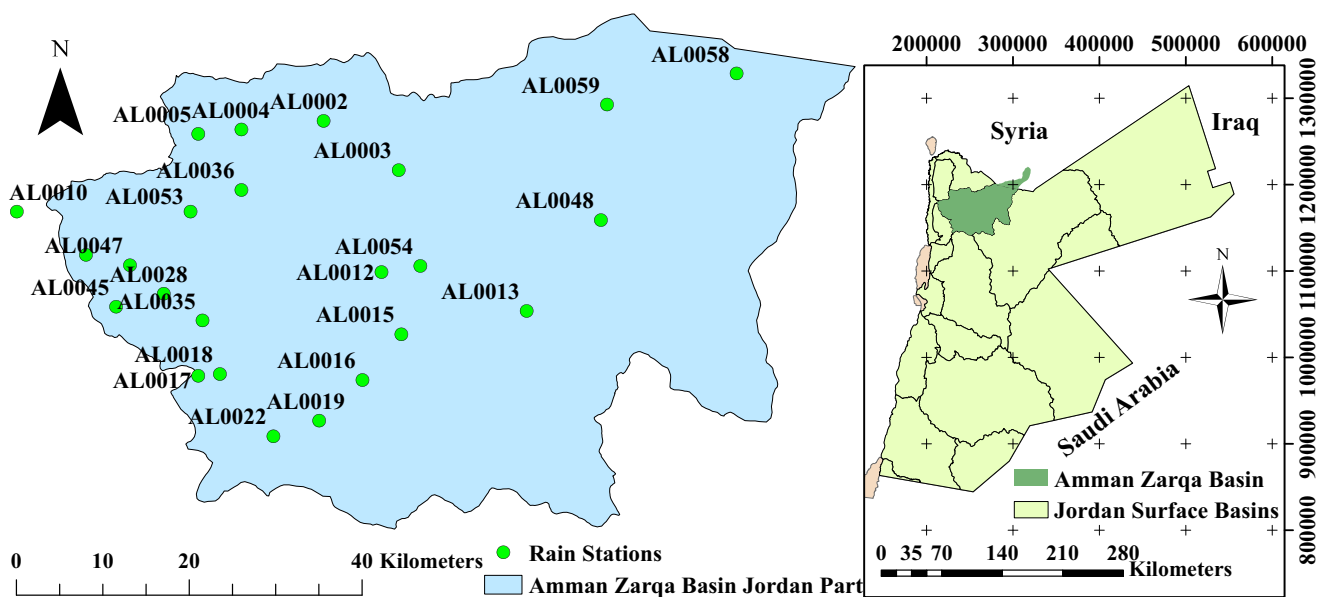


Fig. 1 Amman Zara Basin and the location of weather stations

**Table 1** Selected weather stations basic information (ID, name, coordinates, and elevation) and their statistics based on annual precipitations

No.	Station ID	Station name	Coordinates <sup>a</sup>			Annual precipitation				
			Latitude	Longitude	Elevation	Mean	STD	Skewness	Kurt	CV (%)
1	AL0002	Midwar	1188500	244000	760	230.06	98.00	0.74	0.59	42.6
2	AL0003	Bal'ama	1182800	252700	695	201.68	77.26	0.26	0.07	38.3
3	AL0004	Jarash	1187500	234500	585	350.15	121.65	0.46	0.16	34.7
4	AL0005	Kitta	1187000	229500	665	534.55	186.21	0.16	-0.39	34.8
5	AL0010	Deir Alla agr. station	1178000	208500	-224	269.60	92.13	0.76	0.19	34.2
6	AL0012	Sukhna	1171000	250700	500	145.30	61.41	0.57	0.34	42.3
7	AL0013	Nawasif	1166500	267500	590	126.72	52.07	0.12	-0.67	41.1
8	AL0015	Zara	1163800	253000	610	118.53	61.02	0.19	0.14	51.5
9	AL0016	Ruseifa	1158500	248500	655	147.36	58.34	0.39	0.13	39.6
10	AL0017	Sweilih	1159000	229500	1000	488.85	180.11	0.95	0.89	36.8
11	AL0018	Jubeiha	1159200	232000	980	463.18	165.61	0.38	0.41	35.8
12	AL0019	Amman airport	1153800	243500	790	262.55	92.63	0.42	-0.44	35.3
13	AL0022	Amman Hussein college	1152000	238200	834	373.00	137.82	0.65	0.06	36.9
14	AL0027	Subeihi	1173000	216500	500	403.46	157.87	0.73	1.19	39.1
15	AL0028	Rumeimin	1168500	225500	675	357.90	135.26	0.59	0.80	37.8
16	AL0035	K. H. nursery evap. St. (Baq'a)	1165400	230000	700	327.64	115.33	0.80	1.02	35.2
17	AL0036	Prince Feisal nursery	1180500	234500	300	329.24	131.10	0.79	-0.01	39.8
18	AL0045	Um Jauza	1167000	220000	860	495.72	180.06	0.86	1.73	36.3
19	AL0047	Sihan	1171800	221600	495	378.51	121.58	0.43	-0.55	32.1
20	AL0048	Khaldiya	1177000	276000	630	124.91	62.91	0.92	1.76	50.4
21	AL0053	King Talal Dam	1178000	228600	218	254.62	104.42	0.39	0.91	41.0
22	AL0054	Hashimiya	1171700	255200	550	120.55	50.94	0.40	-0.08	42.3
23	AL0058	Sabha and Subhiyeh	1194000	291800	850	106.17	54.37	0.77	1.01	51.2
24	AL0059	Um El Jumal evap. St.	1190400	276800	650	114.7	47.9	0.2	-0.07	41.7

<sup>a</sup> Palestine coordinates

precipitation whose magnitude exceeds the predefined threshold value for all values of recorded daily precipitation. More details on the selection of the threshold value will be given below in the results and discussion section (i.e., Section 3.1).

## 2.2 The Mann-Kendall test

The Mann-Kendall (M-K) test (Kendall 1975; Mann 1945) is the most widely used nonparametric statistical test for temporal trend detection in meteorological and hydrological data series (Ahmad et al. 2015; Arnone et al. 2013; Atta-ur-Rahman and Dawood 2017; Deni et al. 2010; Douglas and Fairbank 2011; Fiala et al. 2010; Haktanir et al. 2013; Ouarda et al. 2014; Porto de Carvalho et al. 2013; Xia et al. 2012b), such as temperature, precipitation, and streamflow. The test is rank-based, powerful when data are skewed, allows missing values and does not require that the data conform to the normal probability distribution (Yue et al. 2002).

The M-K test involves testing of the hypothesis in which the null hypothesis,  $H_0$ , assumes that the data are independent, identically distributed, and not correlated (i.e., no trend will be

observed). The alternative hypothesis,  $H_a$ , is that the data follow a monotonic trend over time (i.e., there will be either a significant positive or a significant negative trend). The calculation of the M-K test statistics  $S$  and  $V(S)$  and standardized test statistics  $Z^{MK}$  for a time series of  $n$  observation data points are defined as follows (Kendall 1975).

$$S = \sum_{i=1}^{n-1} \sum_{j=i+1}^n \text{sign}(x_j - x_i) \quad (1)$$

where  $S$  computes the difference between a later-measured value and all earlier-measured values,  $(x_j - x_i)$ , by assigning integer values for  $(x_j - x_i)$  as follows:  $(x_j - x_i) = \{1$  for  $(x_j - x_i) > 0$ ;  $0$  for  $(x_j - x_i) = 0$ ; and  $-1$  for  $(x_j - x_i) < 0\}$ .

For large values of  $n$ , the statistic  $S$  is approximately normally distributed (Kendall 1975) with a mean,  $E(S)$  equal to zero, and the variance is given by  $V(S) = \frac{n(n-1)(2n+5)}{18}$ . Therefore, the standardized M-K test statistic  $Z^{MK}$  is given by  $Z^{MK} = \frac{S-1}{\sqrt{V(S)}}$  for  $S > 0$ ,  $Z^{MK} = 0$  for  $S = 0$ , or  $Z^{MK} = \frac{S+1}{\sqrt{V(S)}}$  for  $S < 0$  and follows a standard normal distribution.

The null hypothesis is rejected (i.e., a significant trend exists that is either positive or negative) if  $|Z^{MK}| > Z^{critical}_{1-\alpha/2}$  in a two-sided test. The critical value  $Z^{critical}_{1-\alpha/2}$  determined from the standard normal table at a significance level  $\alpha$  of 0.05 is 1.96. Thus, a positive  $Z^{MK}$  value ( $Z^{MK} > 1.96$ ) denotes a significant increasing trend at the 5% significance level, and a negative value ( $Z^{MK} < -1.96$ ) denotes a significant decreasing trend at the 5% significance level.

### 2.3 Extreme precipitation probability distribution models

In this research, four generalized probability distributions (namely, GEV, GP, GLN, and GLO) are used to fit the AM and POT data series. Table 2 presents the probability density functions (PDFs) and the cumulative density functions (CDFs) of these distributions with their domains. In these distributions, the random variable  $x$  represents an extreme precipitation amount,  $\xi$  is the location parameter,  $\alpha$  is the scale parameter, and  $k$  is the shape parameter.

Fitting each of the aforementioned probability distributions to the observed data set can be accomplished by estimating its parameters (i.e., shape, location, and scale parameters). In this study, parameters are estimated using the  $L$  moment method.

### 2.4 $L$ moment method

The main role of  $L$  moments is in estimating parameters for probability distributions. Additionally,  $L$  moments are considered another way to describe the shape of a probability and data samples (Hosking 1990) (i.e., provide measures of location, dispersion, skewness, and kurtosis).  $L$  moments, as

defined by Hosking (1990) and Hosking and Wallis (1997), appeared to be a modification of probability-weighted moments (PWMs) as proposed by Greenwood et al. (1979). Essentially,  $L$  moments are linear combinations of probability-weighted moments.

The main advantage of  $L$  moments over conventional moments is that the former are linear functions of the data (Hosking 1990). The conventional moment estimators involve squaring, cubing, and quadrupling the observed data, as in the sample variance, sample coefficient of skewness and sample coefficient of kurtosis, respectively, which gives greater weight to observed data far from the mean value, leading to high bias and variance. Thus,  $L$  moment estimators of the dimensionless coefficients of variation and skewness and kurtosis are almost unbiased (Hosking 1990; Stedinger et al. 1993). Additionally,  $L$  moments suffer less from the effects of sampling variability (Hosking 1990) and are therefore not as sensitive to extreme values (maximum and minimum), and  $L$  moment estimates from small samples are subject to small bias. Furthermore, the required computation is quite limited compared with other traditional techniques, such as maximum likelihood and least-squares (Pandey et al. 2001).  $L$  moments are capable of characterizing a wider range of distributions compared to conventional moments. A distribution may be specified by its  $L$  moments, even if some of its conventional moments do not exist (Hosking 1990). Accordingly, the method of  $L$ -moments has found wide application in the field of hydrology, especially in the case of parameter estimation of probability distributions in frequency analysis studies (Gubareva and Gartsman 2010; Li et al. 2014a, b; Rahman et al. 2013; She et al. 2013; Xia et al. 2012b; Yang et al. 2010; Zakaria et al. 2012; Hosking 2006).

**Table 2** The probability density functions (PDF), cumulative distribution function (CDF) and domain for selected extreme probability distribution in this study

Distributions	PDF	CDF	Domain
GEV	$f(x) = \alpha^{-1} e^{-(1-k)y - e^{-y}}$	$F(x) = e^{-e^{-y}}$	$-\infty < x \leq \xi + \alpha/k$ if $k > 0$ $-\infty < x < \infty$ if $k = 0$ $\xi + \alpha/k \leq x < \infty$ if $k < 0$
GP	$f(x) = \alpha^{-1} e^{-(1-k)y}$	$F(x) = 1 - e^{-y}$	$\xi < x \leq \xi + \alpha/k$ if $k > 0$ $\xi \leq x < \infty$ if $k \leq 0$
GLO	$f(x) = \frac{\alpha^{-1} e^{-(1-k)y}}{(1+e^{-y})^2}$	$F(x) = 1 / (1+e^{-y})$	$\infty < x \leq \xi + \alpha/k$ if $k > 0$ $-\infty < x < \infty$ if $k = 0$ $\xi + \alpha/k \leq x < \infty$ if $k < 0$
GLN	$f(x) = \frac{e^{-(y-\xi)^2/2}}{\alpha\sqrt{2\pi}}$	$F(x) = \phi(y)$	$-\infty < x \leq \xi + \alpha/k$ if $k > 0$ $-\infty < x < \infty$ if $k = 0$ $\xi + \alpha/k \leq x < \infty$ if $k < 0$

Where  $\phi(\cdot)$  is cumulative distribution function of standard normal distribution and  $y = \begin{cases} -k^{-1} \ln\{1-k(x-\xi)/\alpha\}, & k \neq 0 \\ (x-\xi)/\alpha, & k = 0 \end{cases}$

In practice,  $L$  moments are estimated using the observation data  $x_{(i)}$  from a finite sample of size  $n$  that have been arranged in ascending order. The first four  $L$  moments are given by  $\lambda_1 = b_0 = \bar{X}$ ,  $\lambda_2 = 2b_1 - b_0$ ,  $\lambda_3 = 6b_2 - 6b_1 + b_0$  and  $\lambda_4 = 20b_3 - 30b_2 + 12b_1 - b_0$ , where  $b_0, b_1, b_2$ , and  $b_3$  are sample unbiased estimators of the PWMs and defined by:

$$b_0 = \sum_{i=1}^n \frac{1}{n} x_{(i)} \quad , \quad b_1 = \sum_{i=2}^n \frac{(i-1)}{n(n-1)} x_{(i)} \quad ,$$

$$b_2 = \sum_{i=3}^n \frac{(i-1)(i-2)}{n(n-1)(n-2)} x_{(i)} \quad ,$$

$$b_3 = \sum_{i=1}^n \frac{(i-1)(i-2)(i-3)}{n(n-1)(n-2)(n-3)} x_{(i)}$$

According to terminology in Hosking (1990),  $\lambda_1$  is the  $L$  location, a measure of central tendency, and represents the mean of the distribution.  $\lambda_2$  is the  $L$  scale, analogous to the

standard deviation. Additionally, other dimensionless quantities called  $L$  moment ratios, defined as  $L$  skewness  $\tau_3$  ( $\tau_3 = \lambda_3/\lambda_2$ ) and  $L$  kurtosis  $\tau_4$  ( $\tau_4 = \lambda_4/\lambda_2$ ), are measures of skewness and kurtosis, respectively. Finally, the dimensionless ratio called the coefficient of  $L$  variation, defined as  $\tau_2$  ( $\tau_2 = \lambda_2/\lambda_1$ ), is analogous to the conventional CV. The estimates of the scale, location, and shape parameters of the GEV, GP, GLO, and GLN distributions by  $L$  moments are given in Table 3 as developed by Hosking (1990).

### 2.5 Return period

In hydrology, the return period ( $T$ ), also known as the average recurrence interval, is a means to express exceedance probabilities. The return period is defined as the average length of time in years in which an event of a given magnitude is to be equaled or exceeded on average once. Mathematically, the return period of an event of a given magnitude is equal to

**Table 3** The  $L$  moments estimates of parameters and predicted precipitation amount associated with return period  $T$  years for selected extreme probability distribution in this study

Distributions	$L$ moments parameters estimators	Predicted rainfall amount associated with return period $T$ years (the quantiles)
GEV	$\hat{k} \approx 7.8590c + 2.9554c^2$ $c = \frac{2}{3+\tau_3} - \frac{\log 2}{\log 3}$ $\hat{\alpha} = \frac{\lambda_2 \hat{k}}{(1-2^{-\hat{k}})\Gamma(1+\hat{k})}$ $\hat{\xi} = \lambda_1 - \alpha \left\{ 1 - \Gamma(1 + \hat{k}) \right\} / \hat{k}$	$X_T = \begin{cases} \hat{\xi} + \frac{\hat{\alpha} \left\{ 1 - (-\ln[1 - \frac{1}{T}])^{\hat{k}} \right\}}{\hat{k}} & , \hat{k} \neq 0 \\ \hat{\xi} - \hat{\alpha} \ln \left( -\ln \left[ 1 - \frac{1}{T} \right] \right) & , \hat{k} = 0 \end{cases}$
GP	$\hat{k} = (1-3\tau_3) / (1+\tau_3)$ $\hat{\alpha} = (1 + \hat{k}) (2 + \hat{k}) \lambda_2$ $\hat{\xi} = \lambda_1 - (2 + \hat{k}) \lambda_2$	$X_T = \begin{cases} \hat{\xi} + \frac{\hat{\alpha} \left\{ 1 - (1 - [1 - \frac{1}{T}])^{\hat{k}} \right\}}{\hat{k}} & , \hat{k} \neq 0 \\ \hat{\xi} - \hat{\alpha} \ln \left( 1 - \left[ 1 - \frac{1}{T} \right] \right) & , \hat{k} = 0 \end{cases}$
GLO	$\hat{k} = -\tau_3$ $\hat{\xi} = \lambda_1 + \frac{(\lambda_2 - \hat{\alpha})}{\hat{k}}$ $\hat{\alpha} = \frac{\lambda_2}{\Gamma(1+\hat{k})\Gamma(1-\hat{k})}$	$X_T = \begin{cases} \hat{\xi} + \frac{\hat{\alpha} \left\{ 1 - [(1 - [1 - \frac{1}{T}]) / [1 - \frac{1}{T}]]^{\hat{k}} \right\}}{\hat{k}} & , \hat{k} \neq 0 \\ \hat{\xi} - \hat{\alpha} \ln \left\{ \left( 1 - \left[ 1 - \frac{1}{T} \right] \right) / \left[ 1 - \frac{1}{T} \right] \right\} & , \hat{k} = 0 \end{cases}$
GLN	$\hat{k} = -\tau_3 \frac{2.0466 - 3.6544\tau_3^2 + 1.8397\tau_3^4 - 0.2036\tau_3^6}{1 - 2.0182\tau_3^2 + 1.242\tau_3^4 - 0.21742\tau_3^6}$ $\hat{\alpha} = \frac{\lambda_2 \hat{k} \exp(-\hat{k}^2/2)}{1 - 2\phi(-\hat{k}/\sqrt{2})}$ $\hat{\xi} = \lambda_1 - \frac{\hat{\alpha}}{\hat{k}} \left( 1 - \exp(-\hat{k}^2/2) \right)$	The quantiles of GLN has no explicit analytical form

Where  $\Gamma()$  is gamma function and  $\phi()$  is cumulative distribution function of standard normal distribution

the reciprocal of the probability of exceedance, expressed as a fraction, of that event; i.e.,  $T = 1/p$ , where  $p$  denotes the exceedance probability  $P(X \geq x)$ . In terms of  $F$ , the cumulative density function evaluated for a particular event is given by  $T = 1/(1 - F)$ . Table 3 gives the precipitation amount (i.e., the quantile) of GEV, GP, and GLO for a specified return period of  $T$  years.

To accomplish the second objective, the best fitted probability distribution among GEC, GLO, GP, and GLN for a particular AM or POT data series was used to predict the precipitation amount at each station when the return period  $T$  was 5, 10, 25, and 50 years.

### 2.6 Assessment of goodness-of-fit

The goodness-of-fit of a probability distribution describes its consistency with an observed data set. Most of the procedures that test goodness-of-fit are presented as special implementations of a more general method of comparing data with a distribution. This kind of comparison can be framed in terms of a hypothesis test in which the null hypothesis ( $H_0$ ) for the test is the hypothesized probability distribution that fits the data adequately at a particular significance level. In this study, nonparametric Kolmogorov-Smirnov (KS) goodness-of-fit tests at the 5% significance level were employed to identify the applicability of the aforementioned probability distributions to fit the AM and POT data series. Moreover, the probability distribution that best fit the data among the applicable distributions was the one with the minimum value of the KS test statistic. In addition, a graphical assessment known as the  $L$  moment ratio diagram was employed to further evaluate whether the AM and POT data series conformed to specific probability distributions.

#### 2.6.1 KS goodness-of-fit test:

The KS goodness-of-fit test is a nonparametric test based on a comparison of the cumulative distribution functions of the hypothesized distribution  $F_0(x)$  and the empirical stepwise distribution  $F_n(x)$  mathematically expressed in Eq. (2) after the data series is sorted in ascending order. The KS test statistic ( $D_n$ ) is the maximum absolute difference between the hypothesized and empirical values of the cumulative distribution over the entire range of  $X$ ,  $D_n = \max |F_0(x) - F_n(x)|$ . The null hypothesis is rejected if the calculated  $D_n$  value exceeds a tabulated critical value ( $D_{n-critical}$ ) for the sample size  $n$  and 5% significance level.

$$F_n(x) = \begin{cases} 0 & , x < x_1 \\ \frac{k}{n} & , x_k < x < x_{k+1} \\ 1 & , x > x_n \end{cases} \quad (2)$$

where  $x_1, x_2, \dots, x_n$  are the values of the ordered extreme precipitation amount and  $k$  is the rank of the precipitation amount in the data series organized in ascending order.

#### 2.6.2 L Moment ratio diagram

The  $L$  moment ratio diagram is a graphical method for the evaluation of the goodness-of-fit. This method was introduced by Hosking (1990) as a useful tool for the selection of a suitable distribution among alternative distribution functions to describe observed data. The  $L$  moment ratio diagram contains the  $L$  kurtosis value ( $\tau_4$ ) plotted against the  $L$  skewness value ( $\tau_3$ ). For various distributions, the theoretical relationship of  $\tau_4$  as a function of  $\tau_3$  is available in the form of polynomial approximation expressions, as suggested by Hosking and Wallis (1997). The  $L$  moment diagram is usually constructed in practical ranges of  $0 < \tau_3 < 0.5$  and  $0 < \tau_4 < 0.4$  (Hosking and Wallis 1997). For the considered distributions in this study, these expressions are given as follows:

$$\tau_4^{GEV} = 0.10701 + 0.11090\tau_3 + 0.84838\tau_3^2 - 0.06669\tau_3^3 + 0.00567\tau_3^4 - 0.04208\tau_3^5 + 0.03763\tau_3^6 \quad (3)$$

$$\tau_4^{GP} = 0.20196\tau_3 + 0.95924\tau_3^2 - 0.20096\tau_3^3 + 0.04061\tau_3^4 \quad (4)$$

$$\tau_4^{GLO} = 0.16667 + 0.83333\tau_3^2 \quad (5)$$

$$\tau_4^{GLN} = 0.12282 + 0.77518\tau_3^2 + 0.12279\tau_3^4 - 0.13638\tau_3^6 + 0.11368\tau_3^8 \quad (6)$$

For each station, the sample estimates of  $L$  skewness ( $t_3$ ) and  $L$  kurtosis ( $t_4$ ) for the AM and POT data series were calculated and represented as point coordinates ( $t_3, t_4$ ) in the  $L$  moment diagram. The best-fitted distribution function can be selected by comparing the vertical distance from the point ( $t_3, t_4$ ), representing the station, to various candidate distribution function curves. The nearest curve to the point (i.e., the minimum vertical distance) can be chosen as the best-fitted distribution function for that station (She et al. 2013; Xia et al. 2012b; Zin and Jemain 2010).

## 3 Results and discussion

### 3.1 POT series threshold selection

The POT series contains all the daily precipitation whose magnitude exceeds a predefined threshold value for all values of recorded daily precipitation. The selection of the most proper threshold value to be used for generating the POT series remains a crucial task. A low threshold value can violate the underlying assumption of the serial independence of POT series (Zin and Jemain 2010), while a high threshold value

will generate few extreme data points, is inadequate for probability distribution parameter estimation (Li et al. 2014a, b) and leads to high variance (Coles 2001). Several methods have been introduced for the selection of an optimal threshold value, such as the percentile value method, mean excess plot method, absolute critical value method, and Hill plot method.

In this study, the threshold is determined by the percentile value method together with the annual average occurrence number (AAON) criterion. AAON is defined as the number of data points in the POT data set divided by the timespan of data (Li et al. 2014a, b). Four POT extreme data series were constructed based on the 90th, 95th, 97.5th, and 99th percentile values. The optimal threshold value is the percentile value corresponding to the POT data series with an AAON criterion between 1 and 2 (Li et al. 2014a, b; Liu et al. 2017). Table 4 shows the potential threshold values based on the percentile method, as well as AAON values at each weather station in AZB. As illustrated, the 95th percentile of the recorded daily precipitation can be considered the optimal precipitation threshold for all weather stations in AZB except for three weather stations, AL0010, AL0018, and AL0019. The 97.5th percentile is a more suitable optimal precipitation threshold for these three stations. These percentile values

(95th and 97.5th) as optimal precipitation thresholds are not surprising results for a semiarid climate region with rare precipitation events, as in AZB. Additionally, as the AAON value increases, the threshold value decreases.

### 3.2 The distribution and variation of AM and POT

Figure 2 illustrates the AM and POT series for the Sweilih (AL0017) and Sabha and Subhiyeh (AL0058) weather stations as an example since these series include the highest and lowest annual precipitation averages, respectively. In the POT series at the Sweilih weather station, the tenth largest precipitation in 1992 was included, and up to the fifth largest precipitation in some other years was also included (i.e., 1951, 1971, and 1991). Additionally, the maximum precipitation amount of 44.5 mm in 2006 is lower than the tenth largest precipitation amount in 1992 of 45.5 mm in the POT series at the Sweilih weather station. Moreover, 21 out of 50 extreme values in the AM series are not included in the POT series for the Sabha and Subhiyeh weather station. These observations confirm previous findings in the literature, for instance (Xia et al. 2012b), that the POT series must also be considered

**Table 4** The precipitation 90th, 95th, 97.5th, and 99th percentile values and AAON values, in curly brackets, at each weather station in AZB

No.	Station ID	90th	95th	97.5th	99th
1	AL0002	20.50 { 2.62}	<b>28.46</b> { 1.30}	38.00 { 0.68}	48.98 { 0.27}
2	AL0003	19.00 { 2.63}	<b>26.00</b> { 1.37}	35.00 { 0.67}	46.00 { 0.29}
3	AL0004	23.14 { 3.75}	<b>33.41</b> { 1.88}	44.96 { 0.95}	56.19 { 0.39}
4	AL0005	39.00 { 3.39}	<b>54.45</b> { 1.68}	68.00 { 0.87}	90.00 { 0.37}
5	AL0010	16.80 { 4.21}	23.40 { 2.11}	<b>31.50</b> { 1.06}	42.00 { 0.44}
6	AL0012	13.00 { 2.82}	<b>18.50</b> { 1.40}	24.09 { 0.70}	31.46 { 0.28}
7	AL0013	13.50 { 2.21}	<b>18.83</b> { 1.11}	23.81 { 0.55}	28.93 { 0.23}
8	AL0015	12.17 { 2.49}	<b>18.00</b> { 1.26}	24.07 { 0.62}	31.57 { 0.26}
9	AL0016	15.00 { 2.46}	<b>21.10</b> { 1.21}	28.93 { 0.61}	36.05 { 0.24}
10	AL0017	32.40 { 3.76}	<b>45.45</b> { 1.89}	59.49 { 0.94}	84.07 { 0.39}
11	AL0018	29.00 { 4.19}	40.00 { 2.30}	<b>52.08</b> { 1.13}	69.96 { 0.49}
12	AL0019	16.30 { 4.47}	24.08 { 2.16}	<b>31.70</b> { 1.09}	42.00 { 0.44}
13	AL0022	27.50 { 3.61}	<b>40.05</b> { 1.79}	51.31 { 0.90}	67.51 { 0.36}
14	AL0027	31.00 { 3.09}	<b>42.50</b> { 1.55}	55.00 { 0.82}	78.40 { 0.31}
15	AL0028	30.00 { 3.15}	<b>41.65</b> { 1.47}	57.79 { 0.75}	72.43 { 0.31}
16	AL0035	23.33 { 3.76}	<b>32.97</b> { 1.89}	40.87 { 0.94}	55.73 { 0.39}
17	AL0036	24.26 { 3.35}	<b>35.00</b> { 1.70}	42.46 { 0.85}	55.19 { 0.35}
18	AL0045	40.00 { 3.20}	<b>53.01</b> { 1.55}	68.73 { 0.78}	93.62 { 0.33}
19	AL0047	28.00 { 3.44}	<b>38.32</b> { 1.68}	45.12 { 0.84}	65.00 { 0.36}
20	AL0048	13.00 { 2.35}	<b>18.00</b> { 1.16}	22.04 { 0.57}	30.19 { 0.24}
21	AL0053	19.80 { 3.18}	<b>27.03</b> { 1.58}	33.00 { 0.84}	40.00 { 0.40}
22	AL0054	11.50 { 2.51}	<b>16.50</b> { 1.31}	20.00 { 0.76}	26.96 { 0.27}
23	AL0058	11.74 { 2.05}	<b>16.00</b> { 1.06}	20.50 { 0.50}	30.00 { 0.22}
24	AL0059	9.00 { 2.94}	<b>12.80</b> { 1.48}	16.00 { 0.78}	21.62 { 0.30}

The bold number is the selected optimal precipitation threshold value correspond to AAON criteria between 1 and 2



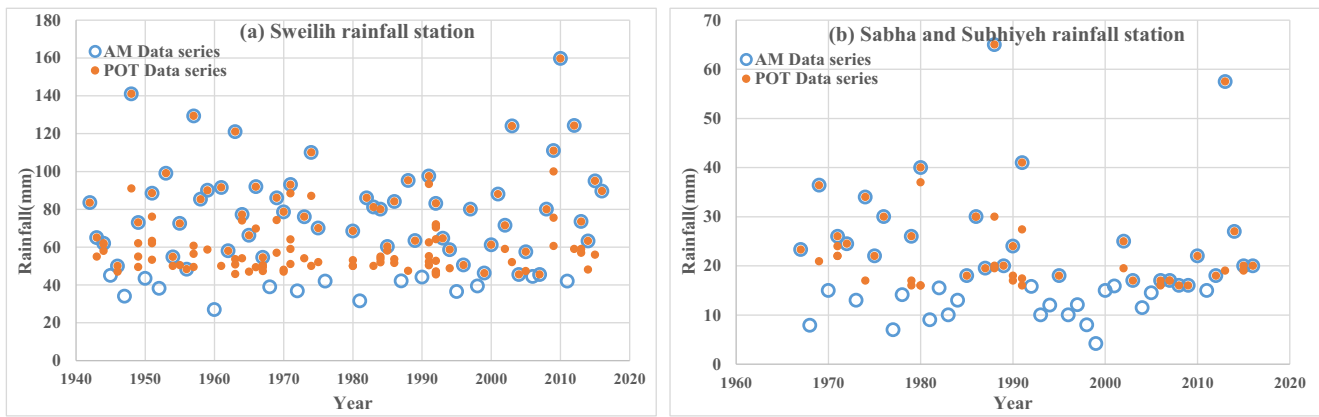


**Fig. 2** AM and POT series of **a** Sweilih weather station (AL0017) and **b** Sabha and Subhiyeh weather station (AL0058)

when precipitation extremes are studied since the POT series provides more information on extremes than the AM series.

Figure 3 depicts the spatial distribution of the mean and the CV of the AM and POT series in AZB. The means (Fig. 3a, b) for both the AM and POT series have similar distributions with east-to-west gradients in which the maximum values are almost observed in the western part and the minimum values are almost observed in the eastern part. From Fig. 3c, d, a similar spatial pattern can be observed for AM and POT for the CV values. Large CV values are almost observed in the northeastern part and

western part of the basin, while minimum values are almost observed in the middle part. Additionally, the values of the CV are larger than 0.37 in the whole area for AM, while for POT, the values are smaller than 0.44 in most of the region. It is also apparent that the mean of the POT series is slightly higher than that of the AM series, which indicates that the POT series considers more information on extremes than the AM series. However, the CV of the AM series is higher than that of the POT series. This suggests that the majority of POT series values are near the threshold level at each station.

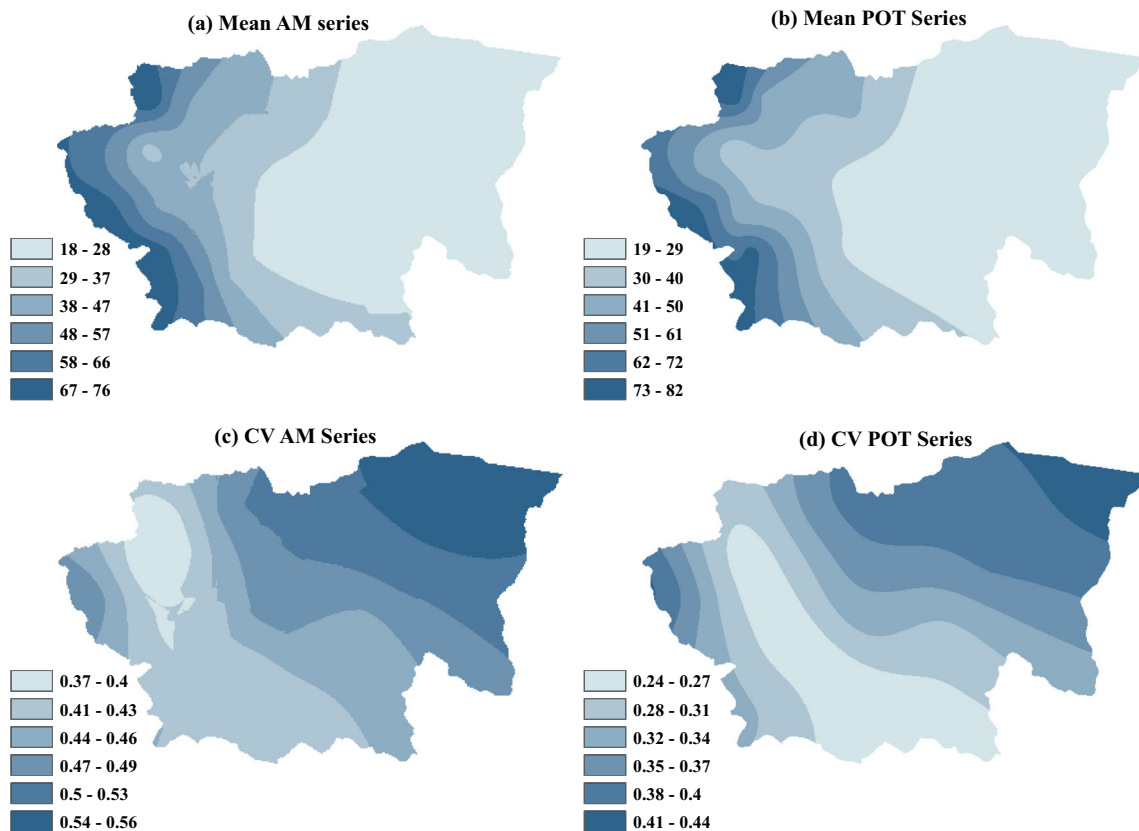


**Fig. 3** The spatial distribution of the mean and the coefficient of variation (CV) of AM and POT series in AZB

### 3.3 Trend analysis of extreme precipitation

Table 5 summarizes the results of the Mann-Kendall (M-K) test. The table shows the test statistic value  $Z^{MK}$  obtained at each station for the annual maximum precipitation (AM) and the POT. The  $Z^{MK}$  values indicate that a mix of increasing and decreasing trends is observed at different stations for both series. However, not all trends are significant. For the AM series, an increasing trend in extreme precipitation is detected at 14 stations, among which three are significant at the 5% significance level (i.e., the null hypothesis  $H_o$  for the M-K test is rejected since  $|Z^{MK}| > 1.96$ ), including AL0002, AL0045, and AL0047. The first station is located in the northern part of AZB, whereas the other two stations are located in the western part of the basin. A decreasing trend is detected at 10 stations. None of these decreasing trends is significant.

Since the POT series considers up to the fifth largest precipitation in some years, in contrast to the AM series, and at the same time skips the largest precipitation in the AM series in other years, the trend analysis results for the POT series

differ slightly from those for the AM series. For the POT series, an increasing trend in extreme precipitation is detected at 16 stations, 4 of which are significant at the 5% significance level. These stations with significant increasing trends include one more station, AL0003, in addition to those stations found by trend analysis of the AM series reported earlier. A decreasing trend is detected at eight stations, among which one station (i.e., AL0054) indicates a significant decreasing trend. In contrast to the AM series, when the POT series is considered, four stations show increasing trends rather than decreasing trends (AL0012, AL0015, AL0019, and AL0053), and two stations show negative trends rather than positive trends (AL0004 and AL0036).

Figure 4 illustrates the results of the M-K test. It is worth noting that increasing-trend stations are mostly found in the western part of the basin, while decreasing trends are found at stations in the northwestern, middle and eastern parts of the basin.

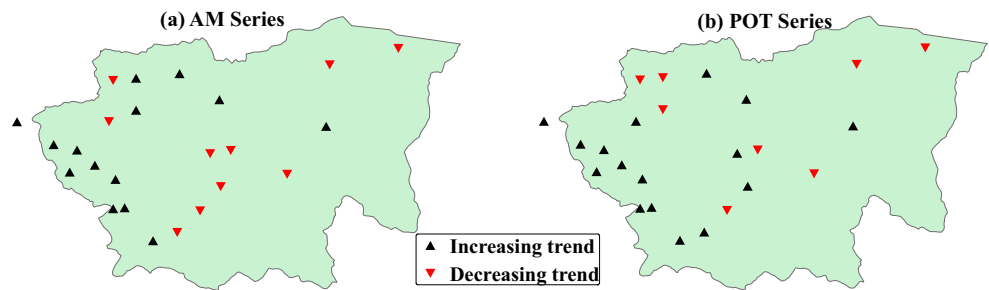
The occurrence date and amount of maximum precipitation for each station throughout the entire study period are

**Table 5** The Mann-Kendall (M-K) test statistic value ( $Z^{MK}$ ) and the Kolmogorov-Smirnov (KS) test statistic value ( $D_n$ ) of AM and POT series for each weather station

Station ID	AM series						POT series					
	M-K Z value	GEV	GLN	GP	GLO	Best distribution	M-K Z value	GEV	GLN	GP	GLO	Best distribution
AL0002	2.16	0.054	0.053	0.118	0.059	GLN	2.82	0.052	0.055	0.065	0.047	GLO
AL0003	0.68	0.067	0.071	<b>0.485</b>	0.062	GLO	2.09	0.070	0.065	0.052	0.076	GP
AL0004	1.26	0.062	0.064	<b>0.236</b>	0.063	GEV	-0.06	0.048	0.048	0.059	0.052	GEV
AL0005	-1.03	0.049	0.050	0.141	0.063	GEV	-0.08	0.108	0.097	0.071	0.122	GP
AL0010	0.62	0.036	0.034	<b>0.179</b>	0.041	GLN	1.03	0.124	0.113	0.085	0.133	GP
AL0012	-1.23	0.065	0.069	<b>0.527</b>	0.053	GLO	0.54	0.077	0.059	0.068	0.083	GLN
AL0013	-1.10	0.049	0.048	0.099	0.059	GLN	-1.25	0.106	0.093	0.065	0.116	GP
AL0015	-0.20	0.081	0.077	<b>0.274</b>	0.096	GLN	0.62	0.121	0.109	0.088	0.130	GP
AL0016	-0.18	0.101	0.103	<b>0.285</b>	0.120	GEV	-0.54	0.050	0.052	0.096	0.060	GEV
AL0017	0.46	0.078	0.077	0.109	0.091	GLN	0.27	0.075	0.062	0.040	0.088	GP
AL0018	1.93	0.069	0.067	0.101	0.066	GLO	0.21	0.070	0.066	0.059	0.078	GP
AL0019	-0.73	0.069	0.043	<b>0.244</b>	0.060	GLN	1.17	0.054	0.052	0.072	0.059	GLN
AL0022	1.47	0.069	0.050	0.157	0.055	GEV	0.51	0.066	0.048	0.056	0.077	GLN
AL0027	1.74	0.069	0.072	0.162	0.093	GLN	1.29	0.074	0.056	0.049	0.083	GP
AL0028	1.45	0.069	0.067	0.183	0.078	GEV	0.49	0.111	0.101	0.069	0.125	GP
AL0035	0.94	0.069	0.056	<b>0.242</b>	0.078	GLN	1.02	0.107	0.092	0.074	0.114	GP
AL0036	0.15	0.069	0.071	0.110	0.092	GLN	-0.39	0.085	0.074	0.059	0.099	GP
AL0045	2.00	0.069	0.083	<b>0.240</b>	0.082	GEV	2.79	0.065	0.051	0.038	0.076	GP
AL0047	2.50	0.069	0.069	<b>0.273</b>	0.095	GLN	2.23	0.120	0.093	0.091	0.128	GP
AL0048	0.91	0.069	0.102	<b>0.332</b>	0.089	GLO	1.07	0.097	0.071	0.068	0.103	GP
AL0053	-0.91	0.069	0.062	<b>0.231</b>	0.047	GLO	0.39	0.090	0.080	0.052	0.102	GP
AL0054	-0.53	0.069	0.065	0.103	0.061	GLO	-2.42	0.109	0.090	0.086	0.114	GP
AL0058	-0.05	0.069	0.072	<b>0.355</b>	0.058	GLO	-1.80	0.088	0.075	0.062	0.095	GP
AL0059	-1.87	0.069	0.059	<b>0.272</b>	0.073	GLN	-1.20	0.088	0.072	0.066	0.098	GP

The bold number means that the null hypothesis ( $H_o$ ) for the KS test is rejected for the hypothesized probability distribution under 5% significance level

**Fig. 4** The spatial distribution of the trends of AM and POT series in AZB



presented in Fig. 5. The highest values are mostly located in the eastern part of AZB, and the smallest values are mostly located in the western part. This accompanies the decrease in elevation and transition from semiarid to arid climate zones. The month with the most frequent occurrence of the maximum precipitation amount at most stations is January, followed by December (10 stations and 8 stations, respectively); these stations are mostly located in the eastern and western parts of AZB. In the middle part of the basin, the occurrence months of maximum precipitation are distributed among December, January, February, and March. Figure 5 further reveals that maximum precipitation events at nine stations occurred after 2009. Eight of these nine stations show positive trend values (refer to the M-K test results in Table 5). Three stations experience a significant trend. This suggests that the number of extreme precipitation events increased slightly in the last decade.

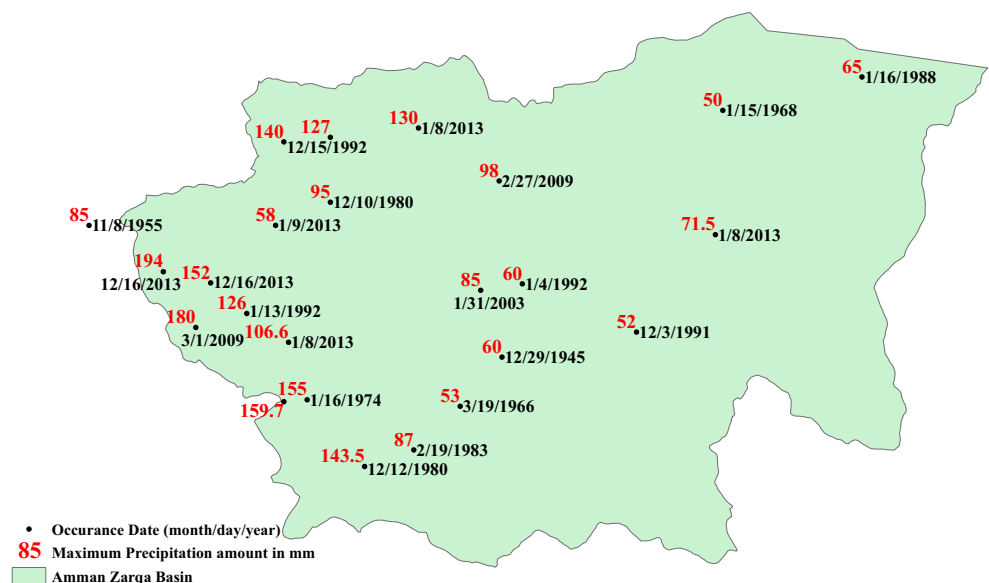
### 3.4 The best-fit probability distribution for extreme precipitation

In this study, both the AM and POT extreme precipitation series are fitted by GEV, GP, GLO, and GLN distributions. The shape, location, and scale parameters for each distribution

are estimated by the  $L$  moment method. Table 5 summarizes the results of the goodness-of-fit test (Kolmogorov-Smirnov (KS) test). The table shows the test statistics value  $D_n$  obtained at each station for the AM and POT series by using the four distributions. The smaller the value of the test statistic  $D_n$ , the better the probability distribution fits the extreme precipitation data series. Table 5 presents the optimal distribution for each station in AZB. Bold values in Table 5 indicate that the probability distribution is not adequate to fit the data series at the 5% significance level (i.e., the null hypothesis  $H_o$  for the KS test is rejected) since the  $D_n$  values are greater than the related critical value ( $D_{n-critical} = 1.36/\sqrt{n}$  for a sample size  $n$  at the 5% significance level).

Based on the KS test (Table 5), for the AM series, out of 24 stations, 11 are best fitted by the GLN distribution, 7 are best fitted by the GLO distribution and 6 are best fitted by the GEV distribution. None of the stations are fitted by the GP distribution. Most distributions passed the KS test at the 5% significance level, indicating that the sample distribution follows the theoretical distribution, except for the GP distribution, which failed to pass the test at 13 stations. However, for the POT series, most stations (18 out of 24) follow the GP distribution. A small number of stations can be better fitted by the GLN, GEV, and GLO distribution (3, 2, and 1 stations, respectively).

**Fig. 5** Occurrence date for maximum precipitation (month/day/year) and its amount in millimeters (number in red color) for each station through entire study period in AZB



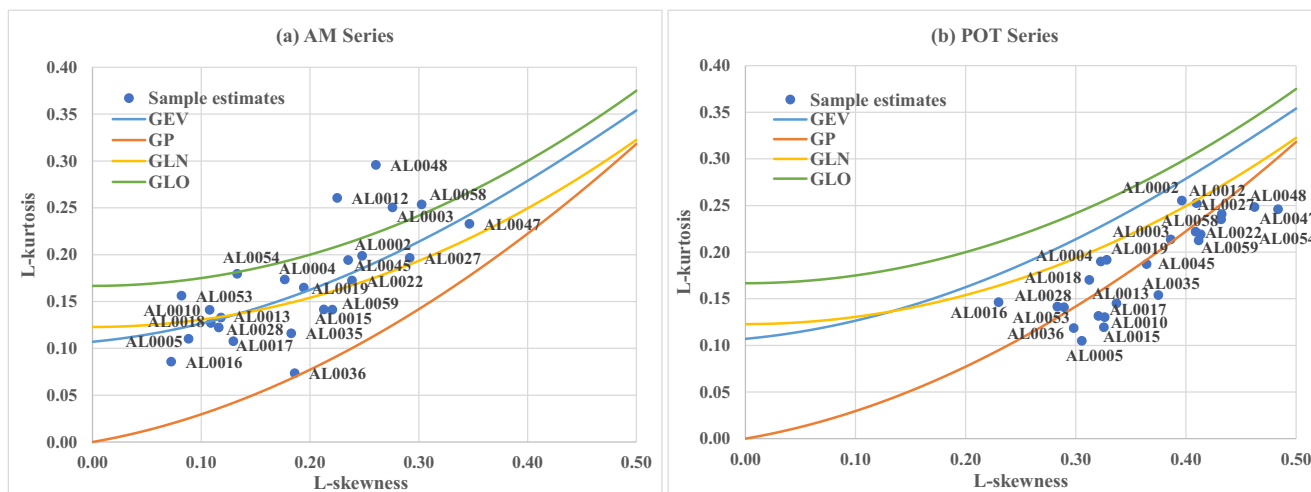


Fig. 6 Sample estimates and theoretical  $L$  skewness and  $L$  kurtosis are compared for a AM and b POT series in the AZB

The four distributions passed the KS test at the 5% significance level.

The graphical method for the evaluation of the optimal distribution through  $L$  moment diagrams is illustrated in Fig. 6. In Fig. 6, the sample estimates and theoretical  $L$  skewness and  $L$  kurtosis are compared for both the AM and POT series. For the AM series, the weather station sample estimates of  $L$  skewness ( $t_3$ ) and  $L$  kurtosis ( $t_4$ ) points ( $t_3, t_4$ ) are scattered widely around the theoretical curves of the four distributions. Based on the criterion that the theoretical distribution curve with the minimum vertical distance will be chosen as the best optimal distribution, the number of stations that can be better fitted by GEV, GLN, GLO, and GP is 9, 7, 7, and 1 out of 24, respectively. For the POT series, most station sample estimate points are concentrated near the GP distribution. There are 19 out of 24 stations that can be better fitted by the GP distribution, and the remaining stations are better fitted by the GLN distribution. No station is fitted by either the GEV distribution or GLO distribution.

The results of the goodness-of-fit tests (KS test and  $L$  moment diagram) suggest that among the GEV, GLN, and

GLO distributions, there is no unique distribution that can be consistently ranked best for all stations using the AM series, while the POT series can be better fitted by the GP distribution in AZB. Figure 7 presents the spatial distribution of best-fitted probability distributions for the (a) AM series and (b) POT series according to the goodness-of-fit KS test results in AZB. There is no clear pattern for the best-fitted distribution connected with any spatial location for the AM series.

The result that the best-fitted distributions vary among the weather stations for the AM series could be due to the uneven spatial variation in AM series characteristics (i.e., mean, standard deviation, skewness and kurtosis) within AZB. These characteristics may influence the effectiveness of the probability distributions to represent precipitation extremes at the considered weather stations. For example, GEV mostly ranks the best for stations with low skewness (0.3 to 1.2) and low kurtosis (− 0.2 to 2.4), while GLO mostly ranks the best for stations with high skewness (1.4 to 2.2) and high kurtosis (2.7 to 7.3). However, the influence of the aforementioned data series characteristics

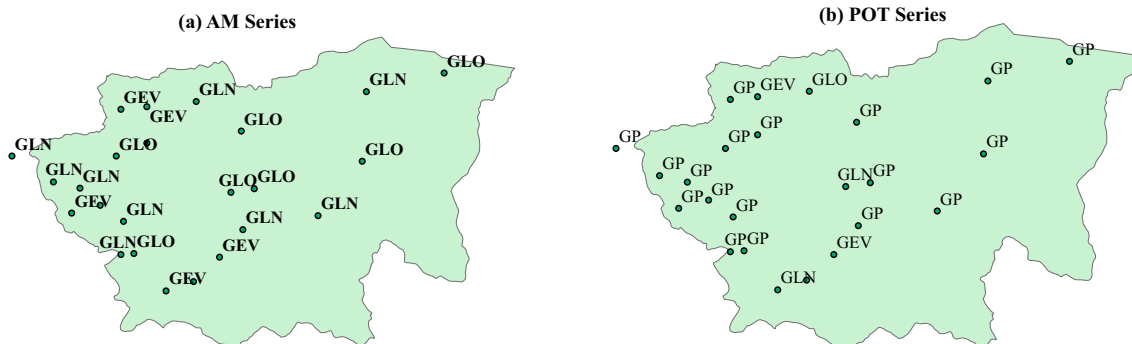
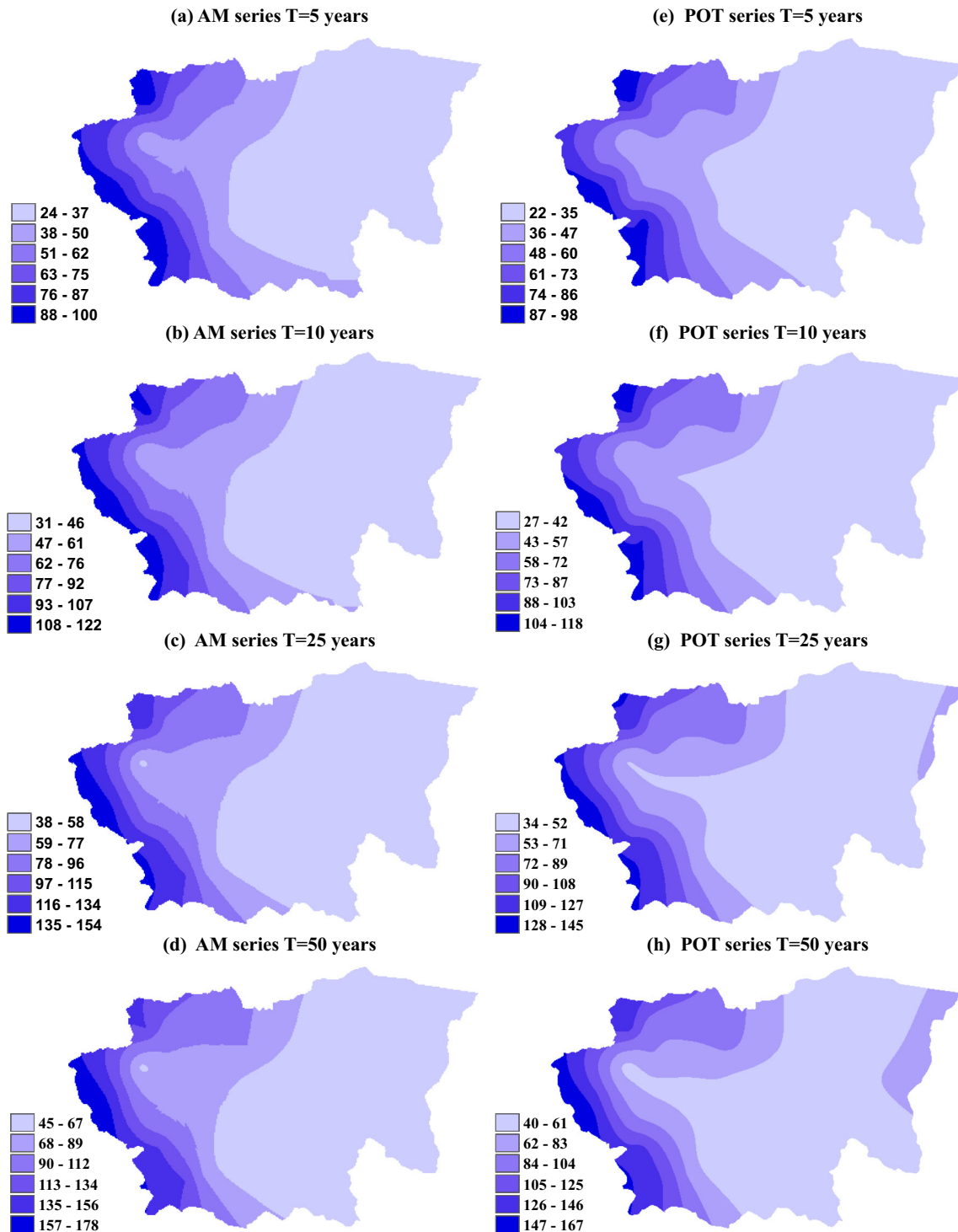


Fig. 7 The spatial distribution of best-fitted probability distribution for a AM series and b POT series according to the goodness-of-fit Kolmogorov-Smimov (KS) test results in the AZB

together with the optimal distribution parameters and the size of the data series should be appropriately investigated in future studies to obtain definitive conclusions. Meanwhile, one can still depend on goodness-of-fit tests (statistical tests or graphical methods) to identify the best distribution among candidate distributions.

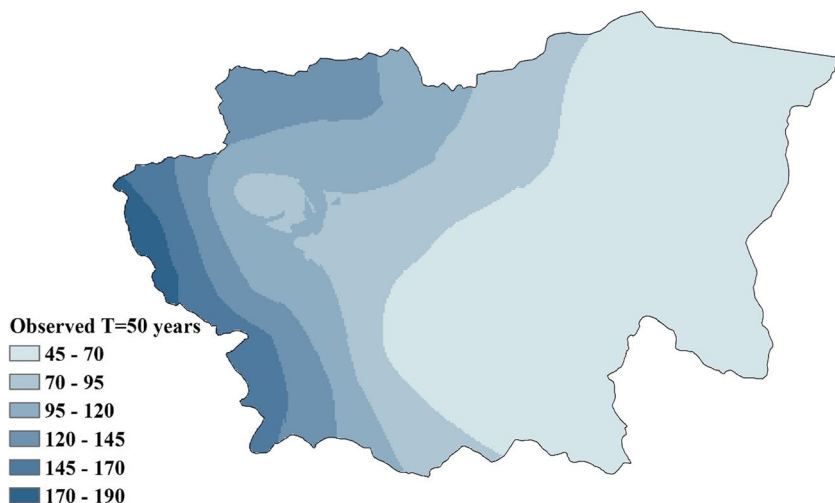
### 3.5 Extreme precipitation estimation under different return periods

After obtaining the optimal distribution at each station, the important question about the occurrence chance of precipitation events larger than a certain amount in any given year in



**Fig. 8** The distribution of calculated extreme precipitations in millimeters under return periods of 5, 10, 25, and 50 years for AM (a–d) and POT (e–h) series using the optimal distribution at each station in the AZB

**Fig. 9** The spatial distribution of observed extreme precipitation in millimeters when the return period is 50 years in the AZB

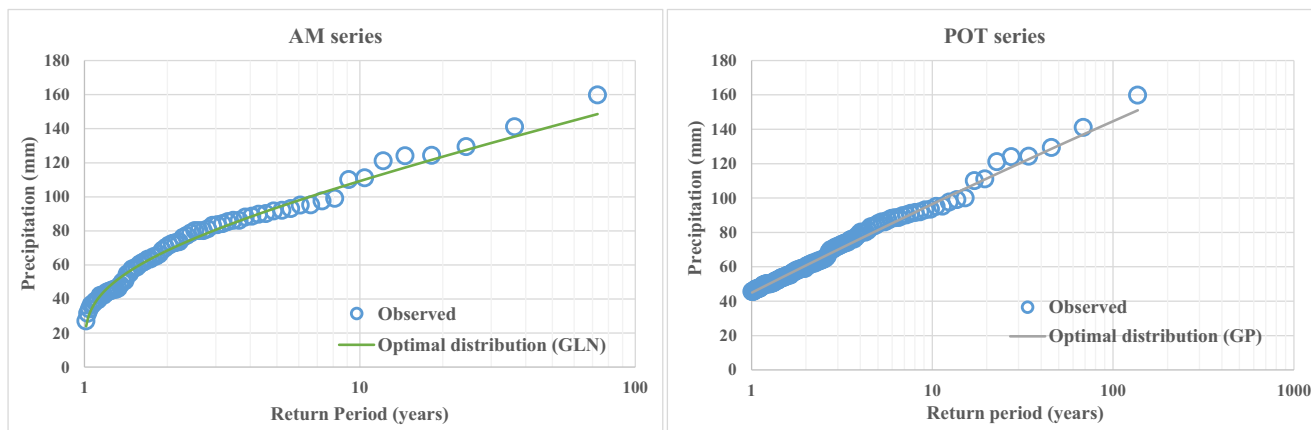


the future can be answered. This is accomplished through return period ( $T$ ) analysis, where the magnitude of an extreme precipitation event is inversely related to its occurrence frequency (i.e., the extreme precipitation value is defined as the maximum value for which the probability that the annual maximum exceeds this value is  $1/T$ ). Therefore, extreme precipitation values under return periods of 5, 10, 25, and 50 years for the AM and POT series using the optimal distribution at each station in the AZB were calculated (equations are given in Table 3) and are illustrated in Fig. 8. For all considered return periods, the spatial variations in extreme precipitation in both the AM and POT series show similar distribution patterns, with decreasing gradients from the west to the east, which is in agreement with the spatial distribution of the means of the AM and POT series given in Fig. 3a, b. Additionally, considering the same return period, the calculated extreme precipitation values of AM are up to 18% greater than those of POT.

Figure 9 presents the spatial distribution of the observed extreme precipitation amount when the return period is 50

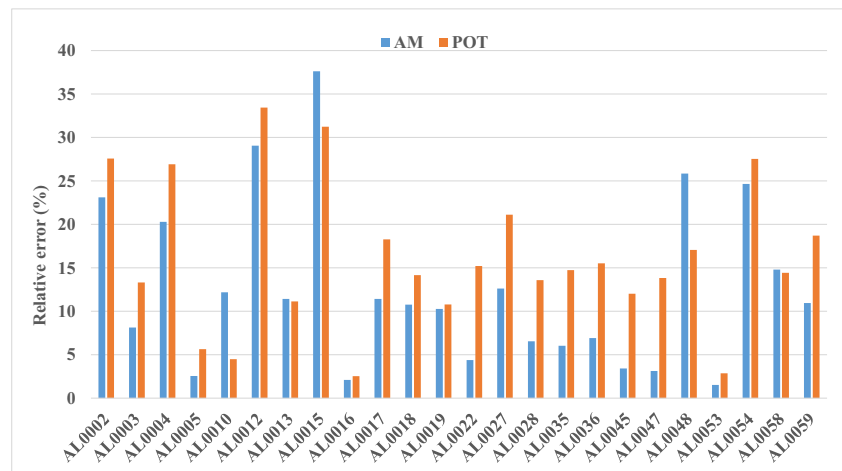
years. In this figure, the maximum observed precipitation amount for each station over the last 50 years is assumed to be the station-observed extreme precipitation value when the return period is 50 years. From a comparison of the calculated extreme precipitation values based on the optimal distribution for both the AM (Fig. 8d) and POT (Fig. 8h) series under a return period of 50 years with the corresponding observed extreme values (Fig. 9), the observed values are higher than the calculated extreme precipitation values of the AM and POT series.

Figure 10 shows the changes in precipitation extremes (i.e., the quantiles or return values) with an increasing return period ( $T$ ) for the Sweilih (AL0017) weather station as an example. In this figure, for both the AM and POT series, the calculated precipitation extremes based on an optimal distribution together with the observed precipitation extremes are represented by the solid line and the circles, respectively. The return periods ( $T$ ) associated with observed precipitation extremes are calculated by the Weibull plotting position formula,  $T = \frac{1}{1 - \frac{i}{n+1}}$ , where  $i$  is the rank of the extreme precipitation



**Fig. 10** Calculated precipitation based on optimal distribution and observed precipitation amount for AM and POT series for AL0017 weather station

**Fig. 11** Relative errors between the calculated and observed extreme precipitation from both AM and POT series at each weather station in AZB when return period is 50 years



amount in the data series organized in ascending order and  $n$  is the length of data series. From this figure, the calculated precipitation amount based on the optimal distribution provides a good match to those observed from the AM and POT series, even for high return periods. Thus, the GLN and GP distributions can fit the observed extremes from the AM and POT series well, respectively, at this particular station (the results of the KS test, Table 5, are used to determine the optimal distribution).

Moreover, the calculated extreme precipitation amount from both the AM and POT series based on the optimal distribution can be compared with the observed value under a 50-year return period in terms of relative error (i.e., the difference between the calculated AM or POT value and the observed value relative to the observed value for a specified return period). The relative error values are illustrated in Fig. 11. From Fig. 11, the relative errors for the AM series are less than those for the POT series at most stations, suggesting that the AM series and the corresponding optimal distributions at each station can better model extreme precipitation events in the AZB than the POT series. Furthermore, no correlation is found between the observed extreme precipitation amounts and the relative error value at each station.

To obtain another representation of extreme precipitation at each station, the calculated extreme precipitation based on the optimal-distribution-fitted AM series for return periods of 10, 25, 50, and 100 years together with the corresponding total exceedance numbers of precipitation extremes during the study period of 1940–2015 are presented in Table 6. From Table 6, most of the extreme precipitation from 1940 to 2015 at each station occurred within 1- to 10-year return periods (data for 1- and 2-year return periods are not shown in Table 6). Moreover, the highest occurrence frequency of 10-year precipitation extremes occurred during 2010–2015, with 19 occurrences out of 81. Additionally, as the return period increases, extreme precipitation becomes rare. A total of 32, 17, and 12 events occurred within 25, 50, and 100 years,

respectively, of precipitation extremes at all stations. For 25-year precipitation extremes, the number of occurrences in the 1980s is quite comparable to that occurring in the 2000s and during 2010 to 2015, with 8, 6, and 7 out of 32 occurrences, respectively. Eight out of 12 events and 8 out of 17 events occurred after 1990 among 100- and 50-year precipitation extremes, respectively. The 17 events for the 50-year return period occurred only at 13 stations, while the 12 events for the 100-year return period occurred at 12 stations. However, for 50- and 100-year extreme precipitation events, each station had at least one extreme precipitation event, either a 50- or 100-year amount, during its recorded data history, except station AL0053. The 50- and 100-year extreme precipitation events have occurred more frequently in recent years (i.e., after 1990) than in previous years. Higher precipitation extremes of 106.6 to 173.8 mm for the 50-year return period are almost observed in the western part of AZB. High precipitation extremes of 127–194 mm for the 100-year return period are almost observed in the western (AL0017, AL0018, and AL0027) and northern (AL0002 and AL0004) parts of AZB. Stations AL0017 and AL0018 are located in the city of Amman, the capital of Jordan.

## 4 Conclusions

In this paper, precipitation extremes are studied in the AZB, Jordan. Daily precipitation records from 24 weather stations spread across the basin during a period that exceeds 50 years (during 1940–2015 for most stations) are used. Two extreme precipitation series (AM and POT); four generalized probability distributions (GEV, GP, GLO, and GLN); and the  $L$  moment method for distribution parameter estimation are used. Based on the results, the following specific conclusions can be drawn:

The trend analysis for the AM and the POT over the time period 1940–2015 indicates that a mix of increasing and decreasing trends is observed at different stations. Since the POT

**Table 6** Calculated extreme precipitations at different return periods and total exceedance numbers of precipitation extremes during the study period

Station ID	5 years	10 years	25 years	50 years	100 years
AL0002	<b>53.42</b> (4) {1964, 2011, 2006}	<b>67.06</b> (4) {2010, 2012, 2005}	<b>85.46</b> (2) {2009, 2002}	<b>99.94</b>	<b>115.04</b> (1) {2013}
AL0003	<b>46.58</b> (3) {1998, 2015, 1997}	<b>57.52</b> (3) {1993, 1966, 1988}	<b>74.46</b> (2) {1991, 2013}	<b>90.02</b> (1) {2009}	<b>108.66</b>
AL0004	<b>64.34</b> (8) {1979, 1988, 2003}	<b>75.76</b> (5) {1971, 2015, 2013}	90.32 (1) {2002}	<b>101.22</b>	<b>112.12</b> (1) {1992}
AL0005	<b>96.28</b> (13) {1938, 1941, 1963}	<b>110.21</b> (3) {1951, 1980, 1942}	<b>125.95</b> (1) {1960}	<b>136.42</b> (2) {1992, 1971}	<b>145.90</b>
AL0010	<b>47.23</b> (8) {1992, 2006, 1964}	<b>54.35</b> (3) {2013, 1980, 2010}	<b>62.76</b> (1) {1986}	<b>68.67</b>	<b>74.33</b> (1) {1955}
AL0012	<b>32.55</b> (7) {1974, 2015, 2010}	<b>39.88</b> (3) {1991, 1988, 1966}	<b>50.75</b> (1) {1980}	<b>60.3</b> (1) {1958}	<b>71.35</b> (1) {2003}
AL0013	<b>30.21</b> (5) {1979, 1986, 1976}	<b>35.43</b> (2) {1966, 1970}	<b>41.65</b> (2) {1985, 1984}	<b>46.06</b>	<b>50.31</b> (1) {1991}
AL0015	<b>31.78</b> (5) {1944, 2010, 1974}	<b>39.04</b> (6) {1948, 1963, 1953}	<b>48.50</b>	<b>55.74</b> (2) {1945, 1961}	<b>63.12</b>
AL0016	<b>35.05</b> (7) {2010, 1988, 1970}	<b>40.1</b> (4) {1944, 1946, 1948}	<b>45.69</b> (1) {1980}	<b>49.32</b>	<b>52.55</b> (1) {1966}
AL0017	<b>93.66</b> (4) {1953, 1991, 1988}	<b>109.25</b> (5) {2012, 2003, 1963}	<b>128.02</b> (2) {1948, 1957}	<b>141.45</b>	<b>154.49</b> (1) {2010}
AL0018	<b>87.47</b> (12) {1963, 2015, 1938}	<b>102.43</b> (2) {1948, 2012}	<b>122.39</b> (4) {1992, 2009, 2010}	<b>138.31</b>	<b>155.00</b> (1) {1974}
AL0019	<b>48.7</b> (8) {2013, 1953, 1979}	<b>57.75</b> (3) {1966, 2015, 1967}	<b>69.33</b> (2) {1948, 1980}	<b>78.06</b> (1) {1938}	<b>86.88</b> (1) {1983}
AL0022	<b>77.31</b> (7) {2009, 1985, 1971}	<b>94.43</b> (3) {2012, 2001, 2013}	<b>118.07</b> (3) {1974, 1992, 2010}	<b>137.19</b> (1) {1980}	<b>157.61</b>
AL0027	<b>86.32</b> (6) {1992, 2008, 1963}	<b>109.72</b> (4) {1996, 2003, 2015}	<b>142.66</b> (1) {2009}	<b>169.53</b>	<b>194.00</b> (1) {2013}
AL0028	<b>77.42</b> (7) {2010, 2000, 2007}	<b>90.92</b> (1) {1980}	<b>106.79</b> (1) {1963}	<b>117.75</b> (2) {1992, 2003}	<b>128.00</b>
AL0035	<b>62.72</b> (4) {2003, 1992, 1983}	<b>74.38</b> (5) {1979, 1986, 2009}	<b>89.14</b> (1) {1980}	<b>100.16</b> (1) {2013}	<b>111.22</b>
AL0036	<b>56.65</b> (8) {1966, 1979, 1988}	<b>66.52</b> (4) {1971, 1992, 2002}	<b>79.05</b>	<b>88.43</b> (1) {1980}	<b>97.85</b>
AL0045	<b>97.12</b> (5) {1980, 1993, 2010}	<b>119.15</b> (1) {1974}	<b>149.44</b> (2) {1992, 2013}	<b>173.83</b> (1) {2009}	<b>199.78</b>
AL0047	<b>74.00</b> (5) {1979, 1980, 2010}	<b>93.49</b> (3) {1992, 2015, 2003}	<b>122.48</b> (1) {2009}	<b>147.24</b> (1) {2013}	<b>174.71</b>
AL0048	<b>27.77</b> (3) {1991, 1985, 1983}	<b>34.22</b> (3) {1974, 1988, 2010}	<b>44.08</b> (1) {2015}	<b>53.02</b>	<b>63.61</b> (1) {2013}
AL0053	<b>41.26</b> (4) {1992, 2000, 1988}	<b>46.57</b> (1) {1980}	<b>53.49</b> (3) {2013, 1970, 1986}	<b>58.88</b>	<b>64.52</b>
AL0054	<b>27.32</b> (7) {1971, 2013, 1973}	<b>32.47</b> (3) {2010, 1972, 1991}	<b>39.49</b>	<b>45.20</b>	<b>51.39</b> (1) {1992}
AL0058	<b>26.32</b> (3) {1976, 1986, 2014}	<b>33.44</b> (4) {1991, 1980, 1969}	<b>44.75</b>	<b>55.38</b> (2) {1988, 2013}	<b>68.35</b>
AL0059	<b>24.46</b> (4) {1985, 2014, 1969}	<b>30.5</b> (6) {1980, 1967, 1979}	<b>38.42</b>	<b>44.52</b> (1) {1968}	<b>50.78</b>

The bold values are the calculated extreme precipitations at different return periods in millimeters followed by the total exceedance numbers in regular brackets and list of exceedance occurrences years in curly brackets. If total exceedance numbers more than three, the years of the first three highest values are shown



series considers up to the fifth largest precipitation in some years, in contrast to the AM series, and skips the largest precipitation in the AM series in other years, the trend analysis results for the POT series differ slightly from those of the AM series. For the AM series, extreme precipitation events at 14 stations, which are mostly found in the western part, show an increasing trend. Among these 14 stations, three are significant at the 5% significance level. The remaining 10 stations, which are mostly found in the middle and eastern parts, show insignificant decreasing trends. For the POT series, an increasing trend in extreme precipitation is detected at 16 stations, 4 of which are significant at the 5% significance level. A decreasing trend is detected at eight stations, among which one station indicates a significant decreasing trend.

According to the Kolmogorov-Smirnov (KS) test and  $L$  moment diagram, the probability distributions GEV, GLN, and GLO can better fit the AM series with no unique distribution among them consistently ranking the best for all stations, while the POT series is better fit by the GP distribution.

The extreme precipitation amounts under return periods of 5, 10, 25 and 50 years for the AM and POT series using the optimal distribution at each station show similar spatial distribution patterns with a decreasing gradient from west to east. Additionally, by considering the same return period, the calculated extreme precipitation amounts of the AM series are up to 18% greater than those of the POT series. The AM series can better model extreme precipitation events than the POT series in AZB since the relative errors between observed values and calculated values for the AM series are less than those for the POT series at most stations.

From the return period analysis, most of the extreme precipitation from 1940 to 2015 at each station occurred within 1- to 10-year return periods. Additionally, as the return period increases, extreme precipitation becomes rare. However, 23 stations experienced at least one extreme precipitation event, either a 50- or 100-year event, during their recorded data history. The 50- and 100-year extreme precipitation events occurred more frequently in recent years. For the 100-year return period, high precipitation extremes of 127–194 mm are almost observed in the western and northern parts of AZB at five stations, two of which are located in the city of Amman, the capital of Jordan.

In terms of application, the findings of this study about the best probability distributions for each of the data series and the prediction of precipitation extremes amounts for several return periods provide important and valuable information for water resources planning and management tasks in AZB and nearby basins in Jordan. Furthermore, these findings can be used to provide a theoretical support to allow the water managers and the policymakers in Jordan for proper actions such as construction of a proper drainage system and construction of flood control structures to control and minimize the risks of large damages caused by frequent precipitation extremes occurred in recent years in AZB.

**Acknowledgments** The author gratefully acknowledges the Ministry of Water and Irrigation in Jordan for providing the required precipitation data.

## References

- Abolverdi J, Khalili D (2010) Development of regional rainfall annual maxima for southwestern Iran by  $L$ -moments. *Water Resour Manag* 24:2501–2526. <https://doi.org/10.1007/s11269-009-9565-4>
- Adamowski K (2000) Regional analysis of annual maximum and partial duration flood data by nonparametric and  $L$ -moment methods. *J Hydrol* 229(3–4):219–231. [https://doi.org/10.1016/S0022-1694\(00\)00156-6](https://doi.org/10.1016/S0022-1694(00)00156-6)
- Ahmad I, Tang D, Wang T, Wang M, Wagan B (2015) Precipitation trends over time using Mann-Kendall and Spearman's rho tests in Swat River Basin, Pakistan. *Adv Meteorol* 2015. <https://doi.org/10.1155/2015/431860>
- Al-hourri Z, Al-omari A, Saleh O, Centre S (2014) Frequency analysis of annual one day maximum rainfall at Amman Zarqa Basin, Jordan. *Civil and Environmental Research* 6(3):44–57
- Arnone E, Pumo D, Viola F, Noto LV, La Loggia G (2013) Rainfall statistics changes in Sicily. *Hydrol Earth Syst Sci* 17(7):2449–2458. <https://doi.org/10.5194/hess-17-2449-2013>
- Atta-ur-Rahman, Dawood M (2017) Spatio-statistical analysis of temperature fluctuation using Mann-Kendall and Sen's slope approach. *Clim Dyn* 48:783–797. <https://doi.org/10.1007/s00382-016-3110-y>
- Babar S, Ramesh H (2014) Analysis of extreme rainfall events over Nethravathi basin. *ISH Journal of Hydraulic Engineering* 20(2): 212–221. <https://doi.org/10.1080/09715010.2013.872353>
- Benyahya L, Gachon P, St-Hilaire A, Laprise R (2014) Frequency analysis of seasonal extreme precipitation in southern Quebec (Canada): an evaluation of regional climate model simulation with respect to two gridded datasets. *Hydrol Res* 45(1):115–133. <https://doi.org/10.2166/nh.2013.066>
- Beskow S, Caldeira TL, Rogério C, Mello D, Faria LC, Alexandre H, Guedes S (2015) Multiparameter probability distributions for heavy rainfall modeling in extreme southern Brazil. *Journal of Hydrology: Regional Studies* 4:123–133. <https://doi.org/10.1016/j.ejrh.2015.06.007>
- Chen YD, Huang G, Shao Q, Xu C (2006) Regional analysis of low flow using  $L$ -moments for Dongjiang basin, South China. *Hydrol Sci J* 51(6):1051–1064
- Chow VT, Maidment DR, Mays Larry W (1988) *Applied Hydrology*. McGraw-Hill, New York
- Coles S (2001) *An introduction to statistical modeling of extreme values*. Springer, London
- Dahamsheh A, Aksoy H (2007) Structural characteristics of annual precipitation data in Jordan. *Theor Appl Climatol* 88(3):201–212. <https://doi.org/10.1007/s00704-006-0247-3>
- Deni SM, Suhaila J, Wan Zin WZ, Jemain AA (2010) Spatial trends of dry spells over Peninsular Malaysia during monsoon seasons. *Theor Appl Climatol* 99(3–4):357–371. <https://doi.org/10.1007/s00704-009-0147-4>
- Douglas EM, Fairbank CA (2011) Is precipitation in northern New England becoming more extreme? Statistical analysis of extreme rainfall in Massachusetts, New Hampshire, and Maine and updated estimates of the 100-year storm. *J Hydrol Eng* 16(3):203–217. [https://doi.org/10.1061/\(ASCE\)HE.1943-5584.0000303](https://doi.org/10.1061/(ASCE)HE.1943-5584.0000303)
- Du H, Xia J, Zeng S, She D, Liu J (2014) Variations and statistical probability characteristic analysis of extreme precipitation events under climate change in Haihe River Basin, China. *Hydrol Process* 28:913–925. <https://doi.org/10.1002/hyp.9606>

- Ellouze M, Abida H (2008) Regional flood frequency analysis in Tunisia: identification of regional distributions. *Water Resour Manag* 22(8): 943–957. <https://doi.org/10.1007/s11269-007-9203-y>
- Fiala T, Ouarda TBMJ, Hladný J (2010) Evolution of low flows in the Czech Republic. *J Hydrol* 393:206–218. <https://doi.org/10.1016/j.jhydrol.2010.08.018>
- Greenwood JA, Landwehr JM, Matalas NC, Wallis JR (1979) Probability weighted moments: definition and relation to parameters of several distributions expressible in inverse form. *Water Resour Res* 15(5): 1049–1054
- Groisman PY, Knight RW, Easterling DR, Karl TR, Hegerl GC, Razuvayev VN (2005) Trends in intense precipitation in the climate record. *J Clim* 18(9):1326–1350. <https://doi.org/10.1175/JCLI3339.1>
- Gubareva TS, Gartsman BI (2010) Estimating distribution parameters of extreme hydrometeorological characteristics by L-moments method. *Water Res* 37(4):437–445. <https://doi.org/10.1134/S0097807810040020>
- Guru N, Jha R (2015) Flood frequency analysis of Tel Basin of Mahanadi River System, India using annual maximum and POT flood data. *Aquatic Procedia* 4:427–434. <https://doi.org/10.1016/j.aqpro.2015.02.057>
- Haddad K, Rahman A (2011) Selection of the best fit flood frequency distribution and parameter estimation procedure: a case study for Tasmania in Australia. *Stoch Env Res Risk A* 25(3):415–428. <https://doi.org/10.1007/s00477-010-0412-1>
- Haktanir T, Bajabaa S, Masoud M (2013) Stochastic analyses of maximum daily rainfall series recorded at two stations across the Mediterranean Sea. *Arab J Geosci* 6(10):3943–3958. <https://doi.org/10.1007/s12517-012-0652-0>
- Hassan B G H, Ping F (2012) Regional rainfall frequency analysis for the Luanhe Basin—by using L-moments and cluster techniques. *APCBEE Procedia* 1(January):126–135. <https://doi.org/10.1016/j.apcbee.2012.03.021>
- Hosking JRM (1990) L-moments: analysis and estimation of distributions using linear combinations of order statistics. *J R Stat Soc Ser B* 52(1):105–124
- Hosking JRM (2006) On the characterization of distributions by their L-moments. *Journal of Statistical Planning and Inference* 136:193–198. <https://doi.org/10.1016/j.jspi.2004.06.004>
- Hosking JRM, Wallis JR (1997) *Regional frequency analysis: an approach based on L-moments*. Cambridge University Press, Cambridge, England
- IPCC (2007) *Climate change 2007: the physical science basis: contribution of working group I to the fourth assessment report of the inter-governmental panel on climate change*. Cambridge University Press, Cambridge
- Kendall MG (1975) *Rank correlation methods*. Griffin, London
- Lenderink G, van Meijgaard E (2008) Increase in hourly precipitation extremes beyond expectations from temperature changes. *Nat Geosci* 1(8):511–514. <https://doi.org/10.1038/ngeo262>
- Li Z, Brissette F, Chen J (2014a) Assessing the applicability of six precipitation probability distribution models on the Loess Plateau of China. *Int J Climatol* 34:462–471. <https://doi.org/10.1002/joc.3699>
- Li Z, Li C, Xu Z, Zhou X (2014b) Frequency analysis of precipitation extremes in Heihe River basin based on generalized Pareto distribution. *Stoch Env Res Risk A* 28(7):1709–1721. <https://doi.org/10.1007/s00477-013-0828-5>
- Li Z, Li Z, Zhao W, Wang Y (2015) Probability modeling of precipitation extremes over two river basins in northwest of China. *Adv Meteorol* 2015. <https://doi.org/10.1155/2015/374127>
- Li Z, Wang Y, Zhao W, Xu Z, Li Z (2016) Frequency analysis of high flow extremes in the Yingluoxia Watershed in Northwest China. *Water* 8(215):1–15. <https://doi.org/10.3390/w8050215>
- Liu B, Chen X, Chen J, Chen X (2017) Impacts of different threshold definition methods on analyzing temporal-spatial features of extreme precipitation in the Pearl River Basin. *Stoch Env Res Risk A* 31(5):1241–1252. <https://doi.org/10.1007/s00477-016-1284-9>
- Ma S, Zhou T, Dai A, Han Z (2015) Observed changes in the distributions of daily precipitation frequency and amount over China from 1960 to 2013. *J Clim* 28(17):6960–6978. <https://doi.org/10.1175/JCLI-D-15-0011.1>
- Madsen H, Rasmussen PF, Rosbjerg D (1997a) Comparison of annual maximum series and partial duration series methods for modeling extreme hydrologic events: 1. At-site modeling. *Water Resour Res* 33(4):747–757
- Madsen H, Pearson CP, Rosbjerg D (1997b) Comparison of annual maximum series and partial duration series methods for modeling extreme hydrologic events: 2. Regional modeling. *Water Resour Res* 33(4):759–769
- Mann HB (1945) Nonparametric tests against trend. *Econometrica* 13(3): 245–259
- Matouq M, El-Hasan T, Al-Bilbisi H, Abdelhadi M, Hindiyeh M, Eslamian S, Duheisat S (2013) The climate change implication on Jordan: a case study using GIS and artificial neural networks for weather forecasting. *Journal of Taibah University for Science* 7(2): 44–55. <https://doi.org/10.1016/j.jtusc.2013.04.001>
- Noto LV, Loggia GL (2009) Use of L-moments approach for regional flood frequency analysis in Sicily, Italy. *Water Resour Manag* 23: 2207–2229. <https://doi.org/10.1007/s11269-008-9378-x>
- Núñez JH, Verbist K, Wallis JR, Schaefer MG, Morales L, Cornelis WM (2011) Regional frequency analysis for mapping drought events in north-central Chile. *J Hydrol* 405:352–366. <https://doi.org/10.1016/j.jhydrol.2011.05.035>
- O’Gorman PA (2015) Precipitation extremes under climate change. *Current Climate Change Reports* 1(2):49–59. <https://doi.org/10.1007/s40641-015-0009-3>
- Ouarda TBMJ, Charron C, Niranjan Kumar K, Marpu PR, Ghedira H, Molini A, Khayal I (2014) Evolution of the rainfall regime in the United Arab Emirates. *J Hydrol* 514:258–270. <https://doi.org/10.1016/j.jhydrol.2014.04.032>
- Pandey MD, Van GPHAJM, Vrijling JK (2001) The estimation of extreme quantiles of wind velocity using L-moments in the peaks-over-threshold approach. *Struct Saf* 23:179–192
- Parida BP, Moalafhi DB (2008) Regional rainfall frequency analysis for Botswana using L-moments and radial basis function network. *Phys Chem Earth* 33(8–13):614–620. <https://doi.org/10.1016/j.pce.2008.06.011>
- Porto de Carvalho JR, Delgado Assad E, Medeiros Evangelista SR, Da Silveira Pinto H (2013) Estimation of dry spells in three Brazilian regions—analysis of extremes. *Atmos Res* 132–133:12–21. <https://doi.org/10.1016/j.atmosres.2013.04.003>
- Rahman AS, Rahman A, Zaman MA, Haddad K, Ahsan A, Imteaz M (2013) A study on selection of probability distributions for at-site flood frequency analysis in Australia. *Nat Hazards* 69(3):1803–1813. <https://doi.org/10.1007/s11069-013-0775-y>
- Saf B (2009) Regional flood frequency analysis using L-moments for the West Mediterranean Region of Turkey. *Water Resour Manag* 23: 531–551. <https://doi.org/10.1007/s11269-008-9287-z>
- Salahat MA, Al-qinna MI (2015) Rainfall fluctuation for exploring desertification and climate change: new aridity classification. *Jordan Journal of Earth and Environmental Sciences* 7(1):27–35
- She D, Xia J, Song J, Du H (2013) Spatio-temporal variation and statistical characteristic of extreme dry spell in Yellow River Basin, China. *Theor Appl Climatol* 112:201–213. <https://doi.org/10.1007/s00704-012-0731-x>
- Stedinger JR, Vogel RM, Foufoula-Georgiou E (1993) Frequency analysis of extreme events, chapter 18. In: Maidment DR (ed) *Handbook of hydrology*. McGraw-Hill, New York
- Törnros T, Menzel L (2014) Addressing drought conditions under current and future climates in the Jordan River region. *Hydrol Earth Syst Sci* 18(1):305–318. <https://doi.org/10.5194/hess-18-305-2014>

- Vahid Rahmani SM, Hutchinson SL, Hutchinson JMS, Anandhi A (2014) Extreme daily rainfall event distribution patterns in Kansas. *J Hydrol Eng* 19(4):707–716. [https://doi.org/10.1061/\(ASCE\)HE](https://doi.org/10.1061/(ASCE)HE)
- Xia J, Du H, Zeng S, She D, Zhang Y, Yan Z, Ye Y (2012a) Temporal and spatial variations and statistical models of extreme runoff in Huaihe River Basin during 1956–2010. *J Geogr Sci* 22(6):1045–1060. <https://doi.org/10.1007/s11442-012-0982-6>
- Xia J, She D, Zhang Y, Du H (2012b) Spatio-temporal trend and statistical distribution of extreme precipitation events in Huaihe River Basin during 1960–2009. *J Geogr Sci* 22(2):195–208. <https://doi.org/10.1007/s11442-012-0921-6>
- Yang T, Xu C-Y, Shao Q-X, Chen X (2010) Regional flood frequency and spatial patterns analysis in the Pearl River Delta region using L-moments approach. *Stoch Env Res Risk A* 24:165–182. <https://doi.org/10.1007/s00477-009-0308-0>
- Yue S, Pilon P, Cavadias G (2002) Power of the Mann-Kendall and Spearman's rho tests for detecting monotonic trends in hydrological series. *J Hydrol* 259:254–271
- Zakaria ZA, Shabri A, Ahmad UN (2012) Regional frequency analysis of extreme rainfalls in the West coast of peninsular Malaysia using partial L-moments. *Water Resour Manag* 26:4417–4433. <https://doi.org/10.1007/s11269-012-0152-8>
- Zin WZW, Jemain AA (2010) Statistical distributions of extreme dry spell in Peninsular Malaysia. *Theor Appl Climatol* 102:253–264. <https://doi.org/10.1007/s00704-010-0254-2>

**Publisher's note** Springer Nature remains neutral with regard to jurisdictional claims in published maps and institutional affiliations.